ACS Biomaterials SCIENCE & ENGINEERING

Article

Cite This: ACS Biomater. Sci. Eng. 2018, 4, 2412−2423

Pulsatile Chemotherapeutic Delivery Profiles Using Magnetically Responsive Hydrogels

Tania T. Emi,[†] Tanner Barnes,[‡] Emma Orton,[‡] Anne Reisch,[‡] Anita E. Tolouei,[†] S. Zahra M. Madani,[†] and Stephen M. Kennedy*[,†,‡]

[†]Department of Chemical Engineering, University of Rhode Island, Kingston, Rhode Island 02881, United States

[‡]Department of Electrical, Computer, and Biomedical Engineering, University of Rhode Island, Kingston, Rhode Island 028881, United States

Supporting Information

ABSTRACT: Pulsatile chemotherapeutic delivery profiles may provide a number advantages by maximizing the anticancer toxicity of chemotherapeutics, reducing off-target side effects, and combating adaptive resistance. While these temporally dynamic deliveries have shown some promise, they have yet to be clinically deployed from implantable hydrogels, whose localized deliveries could further enhance therapeutic outcomes. Here, several pulsatile chemotherapeutic delivery profiles were tested on melanoma cell survival in vitro and compared to constant (flatline) delivery profiles of the same integrated dose. Results indicated that pulsatile delivery profiles were more efficient at killing melanoma cells than flatline deliveries. Furthermore, results suggested that parameters like the duration of drug "on" periods (pulse width), delivery rates during those periods (pulse heights), and the number/frequency of pulses could be used to optimize delivery profiles. Optimization of pulsatile profiles at tumor sites in vivo would require hydrogel materials capable of producing a wide variety of pulsatile profiles (e.g., of different pulse heights, pulse widths, and pulse numbers). This work goes on to demonstrate that magnetically responsive, biphasic ferrogels are capable of producing pulsatile mitoxantrone delivery profiles similar to those tested in vitro. Pulse parameters such as the timing and rate of delivery during "on" periods could be remotely regulated through the use of simple, hand-held magnets. The timing of pulses was controlled simply by deciding when and for how long to magnetically stimulate. The rate of release during pulse "on" periods was a function of the magnetic stimulation frequency. These findings add to the growing evidence that pulsatile chemotherapeutic delivery profiles may be therapeutically beneficial and suggest that magnetically responsive hydrogels could provide useful tools for optimizing and clinically deploying pulsatile chemotherapeutic delivery profiles.

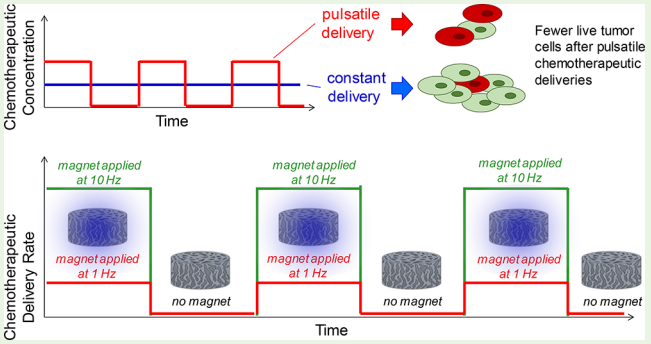

KEYWORDS: *chemotherapy, cancer therapy, responsive hydrogels, smart hydrogels, ferrogels, on-demand drug delivery*

1. INTRODUCTION

Cancer is a widespread family of diseases, causing nearly half a million deaths in the United States in 2016. It is estimated that roughly 40% of American people will be diagnosed with cancer at some point in their life.[1] This motivates the need to develop new cancer treatment strategies. Traditional cancer treatment strategies involve the systemic delivery of chemotherapeutics. However, especially for solid tumors which comprise nearly 85% of cancer cases,[2,3] systemic chemotherapeutic deliveries can have difficulties maintaining drug concentrations at the tumor site and are plagued by off-target side effects.[4,5] Localized deliveries can be achieved from implantable biomaterials and can circumvent some of the aforementioned problems associated with systemic chemotherapeutic deliveries.[4−15] In fact, several biomaterial-based chemotherapeutic treatments are on the market (e.g., Gliadel and Zoladex).[13−16]

While localized chemotherapeutic deliveries from hydrogel implants have yielded promising outcomes, a limitation in their use resides in the fact that the therapeutic concentrations at tumor sites cannot be altered vs time after implantation. This prevents clinicians from altering the course of therapy in response to updates in patient prognosis. Additionally, there is a growing evidence suggesting that the sustained delivery profiles produced by traditional chemotherapeutic-eluding biomaterials (i.e., relatively constant chemotherapeutic concentration vs time) are not optimal. For instance, cancer chronotherapies utilize pulsed chemotherapeutic deliveries to expose cancer cells to higher drug concentrations when they are most susceptible to that drug (e.g., when metabolically active)

Received: March 21, 2018
Accepted: May 15, 2018
Published: May 15, 2018

DOI: 10.1021/acsbiomaterials.8b00348
ACS Biomater. Sci. Eng. 2018, 4, 2412−2423

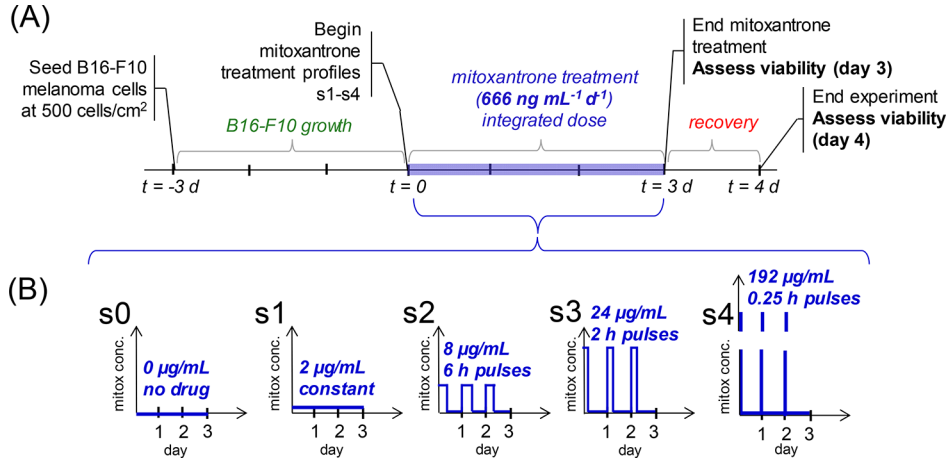

Figure 1. (A) A timeline describing the in vitro cytotoxicity experiment where B16-F10 cells were seeded and allowed to grow for 3 days before treatment, exposed to mitoxantrone treatment profiles s0−s4 for 3 days, and allowed to recover for a day. (B) Delivery schedules (s0−s4) were used on B16-F10 cells where the integrated dose was maintained at 666 ng mL^{-1} day^{-1}.

but when the rest of the body is less susceptible.[17] This approach is based on the fact that tumor cells can exhibit an accelerated metabolic cycle, whereas the rest of the body adheres to a slower, circadian cycle.[18−20] Pulsatile deliveries can also be useful in combating adaptive resistance, a major hurdle in cancer treatment.[21,22] This adaptive resistance may be particularly problematic when using a hydrogel-based approach because they provide cancer cells with an exposure profile that is highly amenable to building resistance (i.e., localized and sustained concentrations). In fact, it has been shown that adaptive resistance can be reduced when chemotherapeutic deliveries are paused and then resumed, a so-called "drug holiday".[21] Taken altogether, these findings suggest that more pulsatile (i.e., periodically on/off) delivery profiles from implantable materials could be advantageous in cancer treatment strategies. While hydrogel materials are highly versatile[23] and can provide localized deliveries,[4] they do not inherently provide pulsatile delivery capabilities.

Stimuli-responsive hydrogels[6] may provide the on-demand control needed to produce localized, pulsatile chemotherapeutic delivery profiles. This class of hydrogels can potentially produce higher delivery rates (establishing higher localized chemotherapeutic concentrations) when subjected to externally applied stimuli (e.g., electrical fields,[24] magnetic fields,[25−32] and ultrasonic signals)[33−35] while producing only baseline levels of release when the stimuli is off. Macroporous alginate ferrogels are of particular interest due to their ability to (i) produce triggered-release profiles in vivo when exposed to the benign magnetic fields emanating from common hand-held magnetics,[25,26] (ii) impede fibrous capsule formation,[36] and (iii) generate temporally complex delivery profiles, even over the course of days to weeks.[37] While showing promise in a number of drug delivery applications, these macroporous ferrogels have not been adapted to deliver the types of pulsatile chemotherapeutic delivery profiles needed to enhance anticancer activity. For example, a common chemotherapeutic installment for treating acute myeloid leukemia involves three days of mitoxantrone delivery,[38] and chronotherapies often involve one chemotherapeutic pulsation per day.[39] However, ferrogels have been limited to pulsatile chemotherapeutic deliveries over the course of hours, not days (i.e., 2 min periods of magnetically enhanced release every half-hour for 3 h total).[25] This study therefore aimed to (i) investigate the impact of different pulsatile chemotherapeutic delivery profiles on cancer cells in vitro over time scales more pertinent to cancer treatment (i.e., 1 pulse per day for 3 days) and (ii) demonstrate the ability to magnetically reproduce multiday, pulsatile delivery profiles using macroporous ferrogels. In pursuit of these aims, this work also addresses other issues arising from attempting to extend pulsatile delivery profiles from hours to days. Namely, this work investigates the use of magnetic field frequency as a means to (i) explicitly regulate the rate of chemotherapeutic release during pulsation and (ii) maintain control over drug delivery rates over time as drug becomes depleted from the gel.

2. MATERIALS AND METHODS

2.1. Materials. B16-F10 mouse melanoma cancer cells were purchased from American Type Culture Collection (ATCC, Manassas, VA). LIVE/DEAD cell imaging kits were purchased from Invitrogen (Carlsbad, CA). Sodium alginate (Protanal LF20/40) of high molecular weight (≈250 kDa) was donated by FMC BioPolymers (Philadelphia, PA). Trypan Blue, MES hydrate, adipic acid dihydrazide (AAD), 1-hydroxybenzotriazole (HOBT), 1-ethyl-3-(dimethylaminopropyl) carbodiimide (EDC), iron (II, III) oxide powder, sodium chloride, activated charcoal, irinotecan hydrochloride, 5-fluorouracil, mitoxantrone, Dulbecco's modified Eagle's medium (DMEM), fetal bovine serum (FBS), penicillin−streptomycin, trypsin−EDTA, and alginate lyase were all purchased from Sigma-Aldrich (St. Louis, MO). Sixteen-well xCELLigence e-plates were purchased from ACEA Biosciences, Inc. (San Diego, CA).

2.2. Cell Culture and Maintenance. B16-F10 mouse melanoma cells were cultured in DMEM with 10% FBS and 1% penicillin−streptomycin at 37 °C in 5% CO_2. B16-F10s were routinely split to avoid confluence over 70%, roughly every other day, by trypsinizing (5 min with 0.25% w/v trypsin and 0.5 mM EDTA), collecting, centrifuging, washing, and reseeding on 75 cm^2 flasks.

2.3. In Vitro Melanoma Cell Survival Studies. Cancer cell survival after flatline (constant) mitoxantrone delivery exposures was compared to that after pulsatile deliveries using B16-F10 mouse melanoma cells in vitro. B16-F10s were seeded at 500 cells per cm^2 on 6-well plates and allowed to grow in DMEM for 3 days before treatment (Figure 1A, $t = -3$ d through 0). Then, for 3 days (Figure 1A, $t = 0$ d through 3 d), B16-F10s were exposed to various mitoxantrone concentrations vs time (Figure 1B, schedules s0−s4). Each of these delivery schedules (s1−s4) utilized the same integrated amount of mitoxantrone (666 ng mL^{-1} day^{-1}). Varying mitoxantrone concentration vs time was achieved by exchanging fresh DMEM with measured concentrations of mitoxantrone in DMEM. When transitioning from mitoxantrone-containing media to mitoxantrone-

DOI: 10.1021/acsbiomaterials.8b00348
ACS Biomater. Sci. Eng. 2018, 4, 2412−2423

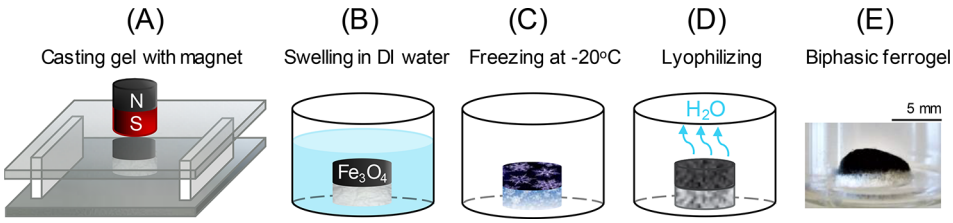

Figure 2. A schematic of the biphasic ferrogel fabrication process. (A) Gels were cast between two glass plates with a magnet on top, (B) allowed to swell in DI water after gel formation, (C) frozen at −20 °C to form ice crystals, and (D) lyophilized to evaporate ice crystals, leaving pores. (E) Photograph of a completed macroporous biphasic ferrogel.

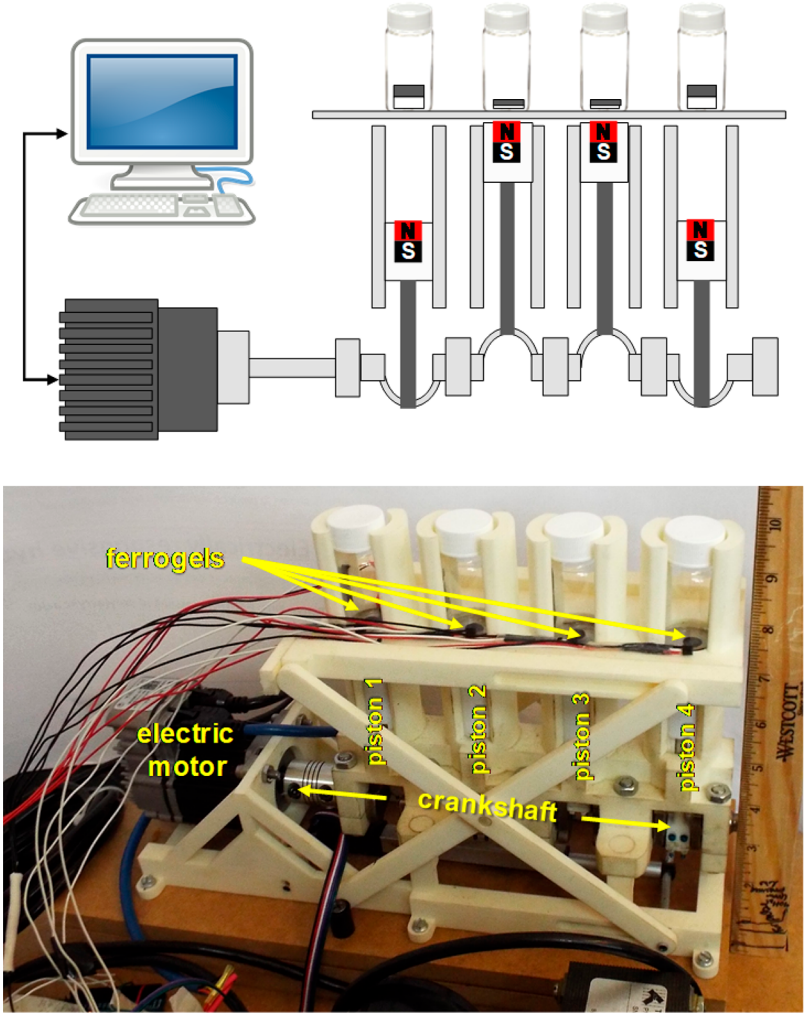

Figure 3. Schematic (top) and photograph (bottom) of the custom magnetic stimulation setup used in these studies.

free media, cells were rinsed 3 times in fresh media to remove any residual mitoxantrone.

After 3 days of treatment, cells were washed 3 times with DMEM so that no residual mitoxantrone was left and allowed to grow for a day in fresh DMEM (Figure 1A, "recovery" t = 3 d through 4 d). Cell viability was quantified on day 3 and day 4 using a LIVE/DEAD staining assay. LIVE/DEAD reagents were added to wells containing cells according to manufacturer protocols (Invitrogen). After 30 min, stained cells were imaged on a BioTek fluorescence imaging plate reader using green/red channels under 4× magnification (enabling the assessment of hundreds to ∼1000 cells per image). BioTek image analysis software was used to tally the number of green-stained (live) cells per image. Each condition s0 through s4 was repeated in 6 separate wells (N = 6) to compute means and standard deviations. Also, culture population was monitored in real-time using 16-well xCELLigence e-plates. E-plate wells (similar in size as 96-well plates) were plated on day −3 at 500 cells per cm^2 and allowed to grow for 3 days (days −3 through 0) before mitoxantrone treatment for 3 more days (days 0 through 3) following the same timeline as provided in Figure 1A. Mitoxantrone concentrations were altered as described above. xCELLigence software was used to collect real-time cell index data for later analysis and plotting. Because cell index values, which represents cell population vs time based on measured impedance, can be variable from experiment to experiment, cell index values were normalized so that values were set to 1 across all conditions at time 0, when mitoxantrone treatment began.

2.4. Biphasic Ferrogel Fabrication. To make magnetically responsive hydrogels, alginate was purified through dialysis (3500 MW cutoff, Spectrum Laboratories, Compton, CA), activated charcoal treatment, filtration, and lyophilization. In a manner previously

DOI: 10.1021/acsbiomaterials.8b00348
ACS Biomater. Sci. Eng. 2018, 4, 2412−2423

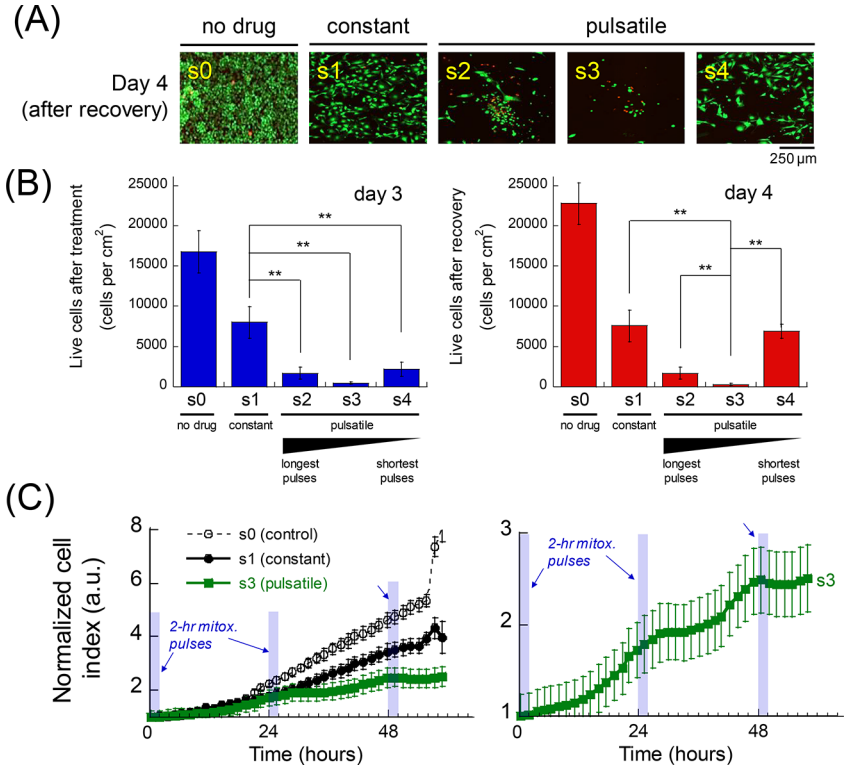

Figure 4. Pulsatile temporal delivery profiles enhance the toxicity of mitoxantrone exposure when compared to constant delivery profiles. (A) Fluorescence microscopy images of B16-F10 cells after LIVE/DEAD (green/red) staining on day 4 after 3 days of exposure to schedules s0−s4 and a day of recovery. (B) Quantification of live cells after the indicated delivery schedules immediately after treatment (left, blue) and after a day of recovery (right, red). $N = 6$. (C) Left: Normalized cell index (melanoma cell population) vs time when exposed to no mitoxantrone (dashed black), constant mitoxantrone concentration (s1, solid black), and a pulsed mitoxantrone profile (s3, solid green). Right: Zoomed-in index vs time for cells exposed to pulsatile schedule s3. Blue rectangles indicate where the mitoxantrone pulses are "on" for the s3 condition. $N = 4$.

described,[26,37] alginate was dissolved in MES buffer (pH = 6.5) with AAD and iron oxide powder to form a solution containing 7 wt % iron oxide, 1 wt % alginate, 2.5 mM AAD cross-linker. Cross-linking was initiated using EDC, and the hydrogels were cast between 2 glass plates spaced 2 mm apart with a magnet placed on top as to pull the iron oxide to one side of the gel, achieving a biphasic structure (Figure 2A). Here, biphasic ferrogel structures were used due to their demonstrated ability to provide higher levels of drug delivery under similar magnetic stimulation conditions when compared to monophasic designs.[26]

After gelation (40 min), individual 8 mm diameter cylindrical gels were cut using a biopsy punch and were rinsed in deionized water for 3 days (exchanging liquid 3 times daily) (Figure 2B). This removed residual reagents from the gel and allowed the gel to swell fully. Gels were then frozen at −20 °C (Figure 2C) and lyophilized (Figure 2D). The resulting structure was an 8 × 2 mm cylindrical dehydrated, macroporous, biphasic ferrogel (Figure 2E).

2.5. Electron Microscopy Imaging of Ferrogels. Structural analyses of freeze-dried ferrogels were performed using scanning electron microscopy (SEM) with a Zeiss SIGMA VP field emission-scanning electron microscope (FE-SEM). Backscattered electron imaging was done using identical conditions at an accelerator voltage of 20 keV and a chamber pressure of 5×10^{-6} Torr. No sputter coating was applied to the ferrogels for imaging. Also, note that because the final steps of the fundamental biphasic ferrogel fabrication involved freezing and lyophilization, no additional freezing/lyophilizing was needed for SEM sample preparation. Thus, SEM sample prep did not generate added porosity to the ferrogels.

2.6. Biphasic Ferrogel Release Studies. Lyophilized ferrogels were loaded with known amounts of mitoxantrone by adding precise volumes of drug solutions to the lyophilized gels. It was determined that ferrogels would absorb no more than 65 μL of liquid. Thus, solutions containing 125 μg of mitoxantrone per 65 μL of PBS were prepared and added dropwise to the iron-oxide-free side of ferrogels (i.e., the white side of the biphasic gel, Figure 2E) and allowed to soak in overnight while sealed in a scintillation vial. This amount of mitoxantrone loading (125 μg per gel) represents an experimentally optimized loading that does not saturate the ferrogel with mitoxantrone (see Supporting Information, Section 1, Figure S1). This lack of saturation reduces the amount of diffusive mitoxantrone release when not magnetically stimulated and enables therapeutically relevant release rates when stimulated (single-digit micrograms per hour). To remove unincorporated mitoxantrone, ferrogels were then soaked in 1 mL of PBS for 1 h. It was found that this method of loading resulted in over 80% of the original 125 μg of mitoxantrone to be taken up by the ferrogels and that subsequent rinsing removed very little beyond that (Figure S2). That is, after loading, an average of 103.3 μg of mitoxantrone was taken up by the ferrogels, and rinsing reduced this amount to an average of 101.4 μg. This amount of mitoxantrone represents the drug contained in the gels prior to release studies and is used to compute the amount of drug remaining (%) vs time. Immediately following rinse, gels were placed in 1 mL of PBS, and the release study was initiated. Ferrogel-containing scintillation vials were placed on top of a custom magnet stimulation system (see next subsection) and exposed to various magnetic stimulation signals (or no signal for control experiments). Samples were taken periodically by fully removing the 1 mL of PBS, reserving it for later analysis, and replacing it with a fresh 1 mL of PBS. The concentration of mitoxantrone contained in collected samples was quantified using BioTek Cytation3 microplate reader to measure optical absorbance at 610 nm for mitoxantrone against a standard curve.

2.7. Custom Magnetic Stimulation System. To expose ferrogels to a wide variety of magnetic stimulation frequencies, a custom magnetic stimulation system was designed and built (Figure 3). This system consisted of an electric motor whose speed could be controlled through a computer interface. This electric motor drove a

DOI: 10.1021/acsbiomaterials.8b00348
ACS Biomater. Sci. Eng. 2018, 4, 2412−2423

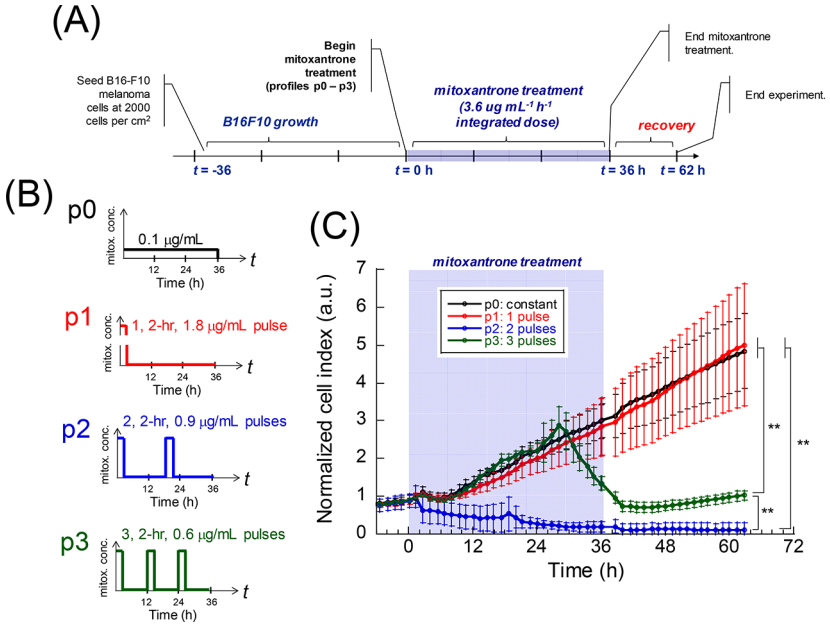

Figure 5. For pulsatile mitoxantrone deliveries, the number of pulses can have an impact on how many melanoma cells survive treatment. (A) A timeline describing the in vitro experiments was conducted. (B) Schematics describing the different pulses mitoxantrone delivery schedules used (0–3 pulses, schedules p0–p3, respectively). (C) Normalized cells index for melanoma cells vs time during mitoxantrone treatment (blue shaded region) and after treatment for cells exposed to schedules p0 (black), p1 (red), p2 (blue), and p3 (green). ** indicates statistically significant differences with $p < 0.01$ as computed using one-way ANOVA with Tukey's post hoc tests for multiple comparisons. $N = 4$.

crankshaft which drove four balanced, in-line pistons. Each piston held a single 1.27 × 1.27 cm cylindrical neodymium magnet (K&J Magnetics, Inc., Pipersville, PA) whose vertical position cyclically raised and lowered as the electric motor ran.

A scintillation vial was held on a platform just above each piston in a manner that held ferrogel samples close to the magnets at maximum height but far enough away to avoid physical contact with the magnet. Thus, four ferrogels could be simultaneously exposed to cyclic magnetic gradients at frequencies prescribed by the motor speed (between 0.01 and 20 Hz). Ferrogel samples contained within their scintillation vials were exposed to between 0 and 5.6 kGauss at piston minimum and maximum positions, respectively, as measured by Hall-effect sensors. Three movies are provided in Supporting Information that shows this device in use at 0.1, 1, and 10 Hz (Movie S1, Movie S2, and Movie S3, respectively).

2.8. Data Representation and Statistical Analyses. All quantitative data presented here are represented by means ± standard deviation, unless otherwise specified. For all statistical analyses, analysis of variance (ANOVA) was used with Tukey's posthoc tests for multiple comparisons (using Kaleidagraph software) and p-values of less than 0.05 being our benchmark for statistical significance. *, **, ***, and **** indicates statistical significance of $p < 0.05$, 0.01, 0.001, and 0.0001 respectively. n.s. indicates no statistical significance. ($p > 0.05$).

3. RESULTS

3.1. Continuous vs Pulsatile Chemotherapeutic Deliveries on Tumor Cells in Vitro. To determine if pulsatile chemotherapeutic deliveries were more toxic to cancer cells than continuous (flatline) deliveries in vitro, B16-F10 mouse melanoma cells were exposed to various mitoxantrone concentration profiles vs time over the course of three days (see Figure 1). Despite using the same integrated doses of mitoxantrone (666 ng mL^{-1} day^{-1}), it was determined that pulsatile delivery schedules could result in lower numbers of live melanoma cells than continuous profiles (Figure 4A). Specifically, immediately after mitoxantrone treatment (Figure 1A, day 3), all three pulsatile delivery schedules tested (schedules s2–s4) resulted in significantly fewer live melanoma cells than the continuous schedule s1 (Figure 4B, left). However, when given a full day to recover after mitoxantrone treatment (Figure 1A, day 4), cells exposed to schedule s4 recovered somewhat (Figure 4B, comparing blue and red bars for s4). Notably though, pulsatile schedules s2 and s3 remained at low levels (Figure 4B, red and blue bars for s2 and s3 remained low).

Pulsatile delivery profiles may have resulted in lower melanoma cell survival than the constant profile due to (i) improved prevention of the cells developing resistance to the drug, but also simply due to (ii) the use of temporary and periodically higher dosing. That is, while the same amount of total drug was used in schedules s1–s4, pulsatile delivery schedules required that higher concentrations be delivered during "on" phases of the delivery profile to match the total integrated dose of the continuous profile. Thus, during these "on" phases, cells were exposed to more toxic concentrations of mitoxantrone. Notably, however, when very toxic/high concentrations were used but for very short "on" periods (i.e., schedule s4: 192 μg/mL but only held for 15 min per "on" period), melanoma cell elimination became less effective (Figure 1B, s4). This could be attributed to there not being a sufficient amount of time for the drug's toxicity to manifest. In the case of this chemotherapeutic, mitoxantrone molecules must be able to internalize and access the cell nucleus where it can disrupt DNA synthesis and repair mechanisms. In fact, mitoxantrone is known to rapidly absorb to tissues[38] with absorption half-lives reported to be on the order of 10 min.[40] Thus, for fleeting drug exposures on the order of that time scale (e.g., 15 min), only a fraction of mitoxantrone would be expected to absorb and have a therapeutic impact on the cells. Of the four mitoxantrone schedules tested, the pulsatile schedule s3 (24 μg/mL held for 2 h per "on" period) yielded the most significant reduction in melanoma cell survival (Figure

DOI: 10.1021/acsbiomaterials.8b00348
ACS Biomater. Sci. Eng. 2018, 4, 2412–2423

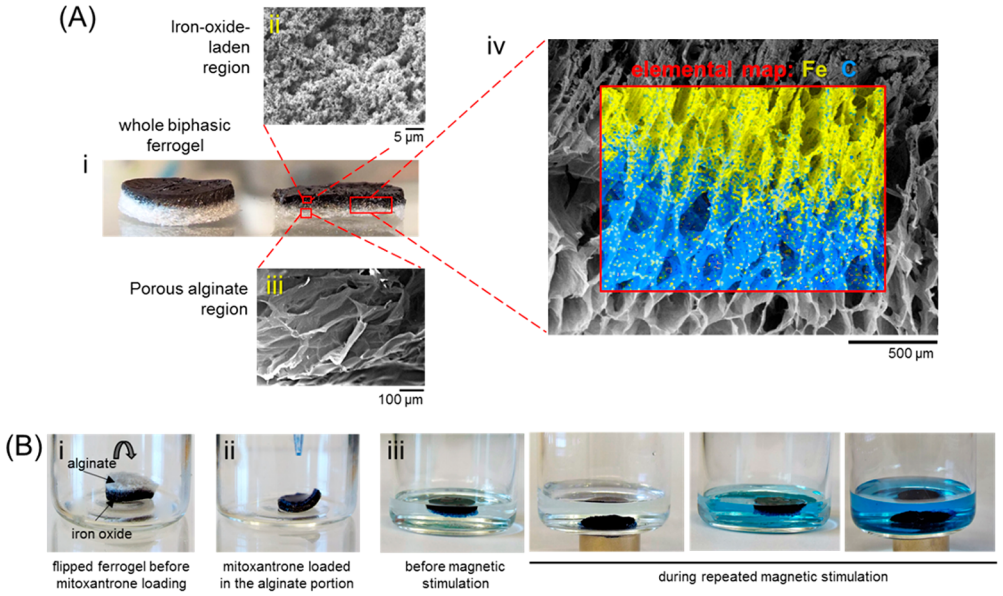

Figure 6. Magnetically responsive biphasic ferrogels were porous in structure and capable of magnetically triggered drug delivery. (A) (i) Photograph of a whole biphasic ferrogel (left) and its cross section (right). SEM images of the iron-oxide-laden region (ii), porous alginate region (iii), and the transition between the two regions (iv). Elemental mapping data show iron (yellow) and carbon (blue). (B) Photographs of a flipped and lyophilized ferrogel prior to drug loading (i), a ferrogel during loading (ii), and a loaded ferrogel being repeatedly stimulated with a hand-held magnet (iii).

4B, right). This may represent a more effective balance of increased mitoxantrone concentrations being held for a sufficiently long period of time (i.e., about 12 half-lives) to reach and interact with intercellular targets.

To examine how these pulsatile deliveries impacted the melanoma cell population in real time during pulsing, similar experiments were conducted on xCELLigence plates: a system that can track cell population (cell index) vs time with a high degree of temporal resolution. As expected, during treatment days 0−3, cell populations exposed to pulsatile deliveries did not reach levels as high as those exposed to constant deliveries (Figure 5C, left, comparing solid green (s3) and solid black (s1) curves). Interestingly, for the pulsatile s3 schedules, melanoma cell populations were most affected during and immediately after mitoxantrone "on" periods (Figure 4C, right). This may indicate that the number of pulses or frequency of pulses in delivery schedules could be used to optimize the efficiency of deliveries. To test how the number/frequency of pulses impacted melanoma cell survival, experiments were conducted where B16-F10s were seeded, allowed to grow, exposed to different mitoxantrone pulsed profiles at the same integrated dose, and left to recover after treatment, all while being monitored for cell index in real time (Figure 5A). Here, pulsatile delivery profiles were either a single pulse (Figure 5B, p1), two pulses (p2), or three pulses (p3), and compared to a constant (flatline) delivery profile (p0). Results indicate significant differences between the number of live melanoma cells remaining after pulsed mitoxantrone treatments with different numbers of 2-h pulses (Figure 5C). In particular, the two-pulse delivery profile (Figure 5C, schedule p2, blue curve) appeared to be the most effective in eliminating melanoma cells. Whiles these effects are the subject of ongoing investigations, schedule p2 may present an effective combination of sufficiently high pulsed dosing repeated enough to be most toxic to melanomas.

Taken together, these data indicate that pulsatile delivery profiles may provide advantages over constant (flatline) delivery profiles. Systemic delivery of pulsatile profiles may be problematic, however, because periodically high concentrations of chemotherapeutics may impose undesirable side effects. These issues could be reduced if deliveries were more localized, for instance, by using a drug-releasing hydrogel implanted at the tumor site. However, traditional hydrogels do not provide pulsatile delivery profiles. This work will therefore investigate if pulsatile deliveries can be administered over the course of several days (mimicking the deliveries here) using magnetically responsive biphasic ferrogels.

3.2. Biphasic Ferrogels for Magnetically Controlled Drug Delivery Profiles. To produce hydrogels capable of generating pulsatile deliveries shown to be effective in vitro, biphasic ferrogels[26,36,37] were fabricated. These cylindrical gels (Figure 6A, i) consisted of an iron-oxide-laden region (Figure 6A, ii) and a soft and deformable porous alginate region (Figure 6A, iii) (see Figure 6A, iv for the transition between these regions). The particular ferrogel formulation used here (7 wt % iron oxide, 1 wt % alginate, 2.5 mM AAD cross-linker, freeze-dried at −20 °C) was previously optimized to provide maximal deformation and drug delivery when exposed to hand-held magnets.[26] After lyophilization, these ferrogels' alginate regions could absorb concentrated solutions of mitoxantrone (Figure 6B, i and ii, mitoxantrone is dark blue). Ferrogels were capable of releasing loaded mitoxantrone earnestly when magnetically compressed with a hand-held magnet and returned to their original shape between compressions (Figure 6B, iii).

3.3. Generation of Pulsatile Mitoxantrone Profiles from Biphasic Ferrogels. Biphasic ferrogels were loaded with mitoxantrone and periodically stimulated with magnetic signals to generate pulsatile delivery profiles. Specifically, the strategy adopted here was to (i) magnetically stimulate at 1 Hz (i.e., 1 magnetic compression per second) during "on" periods to generative temporarily higher mitoxantrone release rates and (ii) not magnetically stimulate during "off" periods to generate lower mitoxantrone release rates (Figure 7A). This magnetic stimulation profile did result in periodically higher mitoxan-

DOI: 10.1021/acsbiomaterials.8b00348
ACS Biomater. Sci. Eng. 2018, 4, 2412−2423

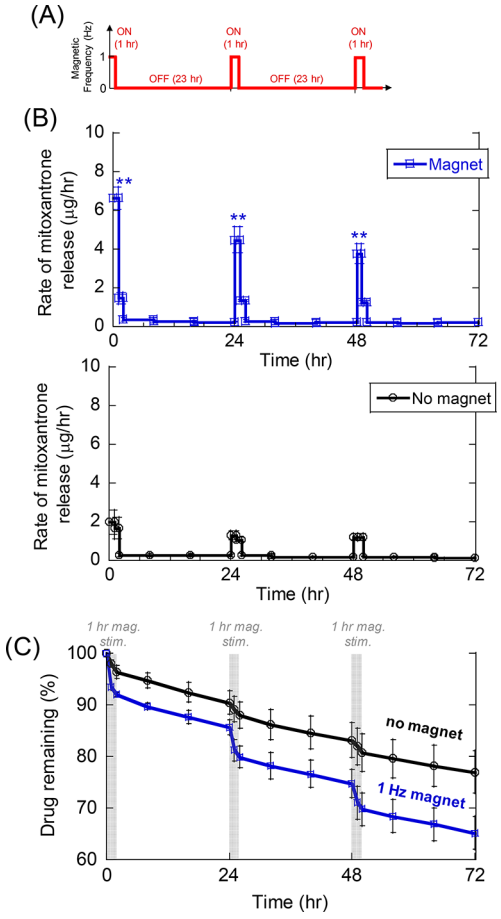

Figure 7. Biphasic ferrogels generate pulsatile delivery profiles when periodically stimulated with hand-held magnets. (A) Schematic of the 1 Hz magnetic frequency stimulation profile used. (B) Mitoxantrone release rate vs time for magnetically stimulated ferrogels (blue) compared to unstimulated controls (black). ** indicates statistical differences relative to controls ($p < 0.01$). (C) Percent of mitoxantrone remaining in ferrogels vs time for stimulated (blue) and unstimulated (black) ferrogels. $N = 4$.

trone release rates as compared to control ferrogels that were not magnetically stimulated (Figure 7B, comparing the height of blue and black curves during "on" periods). Note that even control ferrogels exhibited slightly increased release rates during "on" periods, even though no magnetic stimulation was applied during these times. This was attributed to the agitation associated with removing and adding fresh media during sample collection and reestablished concentration gradients across the perimeter of the gels when fresh media was added. Nevertheless, magnetic stimulation still resulted in statistically significant increases in mitoxantrone release rate during each "on" periods compared to controls (Figure 7B, $p < 0.01$ at 0, 24, and 48 h). While these data show promise, one observed issue was that the magnetically triggered "on" release rates were not consistently high on subsequent days. That is, the release rate achieved through magnetic stimulation deceased each day, despite being stimulated with the same stimulations on each day (Figure 7B, blue curve, descending pulse height at 0, 24, and 48 h). This was attributed to the depletion of mitoxantrone remaining in the gel over time (Figure 7C). As time progressed, less mitoxantrone was available to be magnetically squeezed out of the gel, therefore generating lower release rates when magnetically stimulated. This depletion issue will be addressed in the following subsection. The other observed issue was that the release rates during "on" periods were not explicitly controlled. That is, magnetic stimulation generally enhanced release rates, but the degree of this enhancement was not dictated by the magnetic stimuli. This will be addressed in the next subsection.

3.4. Regulating Chemotherapeutic Release Rate Using the Frequency of Magnetic Stimulation. The ability to remotely regulate the release rate of chemotherapeutics during "on" periods would be very desirable as it would enhance the ability to control the release characteristics after implantation. It was hypothesized that stimulating at higher frequencies would increase the rate of release. That is, when compressed more times within a given window of time, more drug would be convectively purged from the ferrogel. Therefore, the frequency of magnetic stimulation could potentially be used as a way to remotely regulate the rate of release. To test this hypothesis, biphasic ferrogels were loaded with mitoxantrone and stimulated for 10 min at different magnetic frequencies. It was determined that increasing frequencies from 0.1 to 10 Hz did increase the amount of mitoxantrone released (Figure 8).

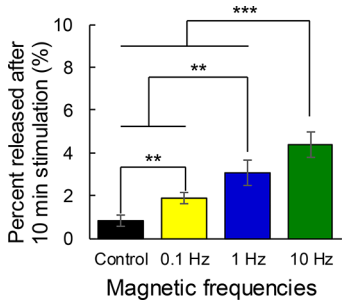

Figure 8. Rate of release can be regulated by stimulating at different frequencies. Percent of drug released after 10 min of magnetic stimulation at the indicated magnetic stimulations: no magnetic stimulation control (black), 0.1 Hz (yellow), 1 Hz (blue), and 10 Hz (green). $N = 4$.

On the basis of these results, it was also hypothesized that the frequency of magnetic stimulation could be used to generate different release rates during "on" phases of a pulsatile delivery schedule. In other words, it was thought that frequency could be used to remotely regulate pulse "height." To test this, experiments similar to those presented in Figure 7 were conducted using frequencies of 0.1, 1, and 10 Hz used during "on" periods (Figure 9A). During the first "on" period, different magnetic stimulation frequencies resulted in statistically different release rates (Figure 9B, day 1 results). However, during subsequent "on" periods, the use of different frequencies to generate different release rates became progressively less effective (Figure 9B, day 2 and day 3 results). In fact, by the time the day 3 "on" period was magnetically triggered, there was no statistical difference between any condition (Figure 9B, day 3 results). This effect was attributed to, again, depletion of available mitoxantrone in the gels. As time progressed, less mitoxantrone was available for release (Figure 9C), making it more difficult to magnetically purge drug for all stimulation frequencies.

3.5. Pulsatile Delivery Schedules with Consistent "On" Period Release Rates vs Time. Because mitoxantrone could be more efficiently released when using higher stimulation

DOI: 10.1021/acsbiomaterials.8b00348
ACS Biomater. Sci. Eng. 2018, 4, 2412−2423

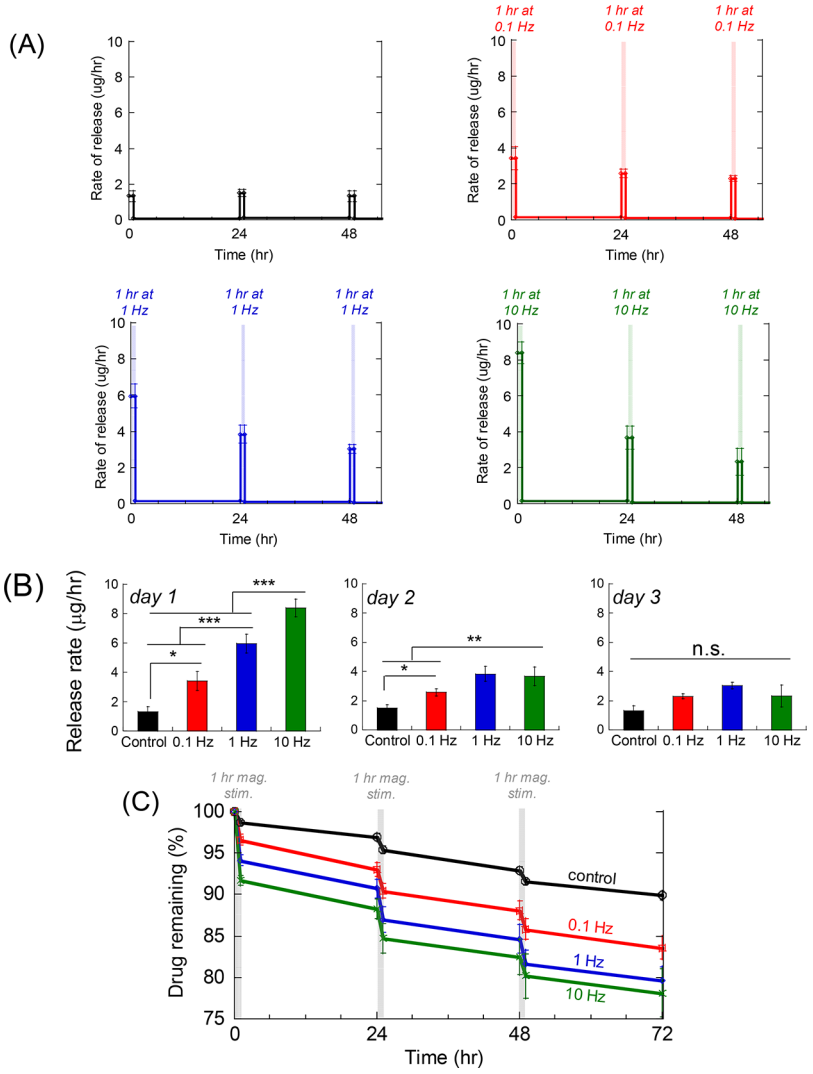

Figure 9. Stimulation at different frequencies yielded different release rates during "on" periods initially, but significant differences were not achieved at later time points. (A) Mitoxantrone release rate vs time for ferrogels exposed to no stimulation (black), 0.1 Hz (red), 1 Hz (blue), and 10 Hz (green) at the indicated times (red, blue, and green shaded regions, respectively). (B) Mean and standard deviation of release rates during "on" periods for days 1 (left), 2 (middle), and 3 (right) for the same conditions shown in part A. (C) Percent of mitoxantrone remaining in gels vs time for the same conditions shown in part (A). $N = 4$.

frequencies, it was thought that higher stimulation frequencies could be used to compensate for reduced release rates as time progressed due to drug depletion. Specifically, the strategy was to use progressively higher stimulation frequencies to maintain more consistent release rates as the drug became more difficult to magnetically purge from the gel (due to there being a less available drug). Therefore, experiments were conducted where subsequent "on" periods used stimulation frequencies of 0.08, 0.8, and 8 Hz (Figure 10A). This progressive magnetic stimulation profile resulted in pulsatile mitoxantrone delivery profiles with consistent pulse heights (Figure 10B). These "on" period release rates were statistically similar on days 1−3 and each higher than controls (Figure 10C). Likewise, the amount of drug remaining in the gels more consistently dropped during subsequent stimulations (Figure 10D, drops during times shaded in gray).

3.6. Extending the Duration of Pulsatile Deliveries from Ferrogels beyond Three Days. While the 3-day pulsatile profiles used in these in vitro studies (Figure 1B) and those generated magnetically from ferrogels (Figure 10B) were based on (i) existing mitoxantrone chemotherapies (e.g., a recommended treatment for acute myeloid leukemia involves 3-day mitoxantrone delivery installments)[38] and (ii) the fact that chronotherapies often involve one chemotherapeutic pulse per day,[39] other emerging therapies could require pulsed delivery profiles extending beyond 3 days. Thus, to investigate ferrogels' abilities to produce pulsatile mitoxantrone delivery profiles for durations longer than 3 days, a magnetic stimulation profile was tested that used progressively higher magnetic stimulation frequencies on subsequent days over the course of 8 days (Figure 11A). Note, however, that the magnetic stimulation setup (Figure 3) permitted only stimulations up to 10 Hz (requiring the electric motor to run at 600 rpm). Thus, on days 4 through 8, magnetic stimulation frequency was maxed out at 10 Hz. Nonetheless, magnetically triggered pulse heights were statistically higher than control gels through day 7 and statistically indifferent from each other through day 5 (Figure 11B). Note that elsewhere, increased mitoxantrone release rates have been delivered from biphasic ferrogels at frequencies up to 40 Hz using electromagnets (without moving parts) to generate

DOI: 10.1021/acsbiomaterials.8b00348
ACS Biomater. Sci. Eng. 2018, 4, 2412−2423

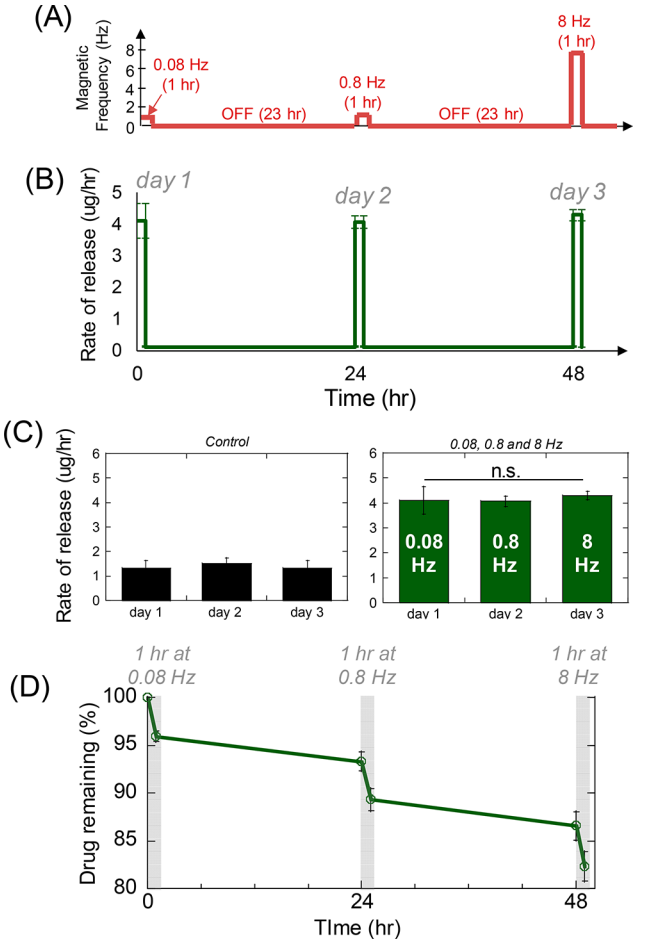

Figure 10. "On" period release rates could be more consistent vs time when progressively higher stimulation frequencies were used. (A) Schematic of the magnetic stimulation profile used. (B) Release rate vs time when subjected to the magnetic stimulation profile described in part A. (C) Releaser rates during "on" periods on days 1, 2, and 3 for unstimulated control gels (black) and gels exposed to the progressive stimulation profile (green). (D) Percent of mitoxantrone remaining in the gels vs time. $N = 4$.

these higher frequencies.[37] Thus, it may be possible to compensate for drug depletion for longer durations than achieved here by continuing to progressively increase stimulation frequency beyond 10 Hz. Also note that though the day-8 magnetically triggered pulse did not meet our benchmark for being statistically higher than controls, it did exhibit a modestly low p-value ($p = 0.057$). On day 8, some of the ferrogels began losing their structural integrity after being so aggressively stimulated on subsequent days (5 days straight at 10 Hz). This loss of structure likely enabled more drug release from some of the gels, thus leading to higher standard deviations in the release data and thus a lack of statistically significant differences when compared to controls. Future ferrogel designs will have to be more robust to facilitate the delivery of prolonged pulsed profiles (i.e., those lasting weeks), though gels held up amply during 3-day pulsatile deliveries, which were shown to be very effective against melanoma cells in vitro (Figure 4).

4. DISCUSSION

These studies demonstrate that pulsatile delivery schedules could provide enhancements in the anticancer activity of chemotherapeutics and that magnetically responsive hydrogels could be used to locally deliver these types of pulsatile schedules. The in vitro findings here that pulsatile delivery profiles are more effective in eliminating cancer cells than constant profiles of the same integrated dose are consistent with (i) other studies that have found that short bursts of high mitoxantrone concentrations are more effective in destroying breast cancer cells,[33] (ii) findings that cancer cells respond to drug exposures more dynamically than once thought,[18,41] and (iii) indications that dynamical drug exposures can have significant impact on cellular responses.[42] If delivered in vivo, pulsatile drug scheduling may also enjoy some of the added benefits associated with chronotherapies. For example, pulsing drug concentrations may be a more effective means to deliver toxins when tumor cells are most susceptible to the drug and while off-target tissues are less susceptible.[17−20] Also, turning drug concentrations on and off may be useful in combatting adaptive resistance.[21] While the work presented here adds to the growing evidence that pulsatile delivery schedules are beneficial, it is important to note that the specific delivery profiles examined here do not represent full optimizations, and these in vitro results cannot be directly translated to effects in vivo. Namely, more complete optimizations will require testing a wider range of pulsatile profiles with different "on" period delivery rates (pulse heights), "on" period durations (pulse widths), and frequencies of pulsing. Optimizations will also need to be tested using other therapeutics, in other cancer cell models (both 2D and 3D models), and in vivo, though systemic delivery of these pulsatile profiles would likely pose problems because periodic overdosing could exacerbate off-target side effects. This motivates the need for implantable drug-delivery materials capable of delivering pulsatile profiles locally at tumor sites. This, in turn, requires hydrogels that can generate a wide variety of different pulsatile delivery schedules (i.e., various pulse widths/heights and frequencies) so that delivery schedules can be experimentally optimized.

The magnetically responsive hydrogels developed here were capable of producing pulsatile mitoxantrone delivery profiles similar to those tested on melanoma cells in vitro (i.e., pulsed over the course of 3 days). Critically, pulsatile delivery parameters such as the timing and delivery rates of pulses could be remotely controlled using magnetic fields emanating from simple hand-held magnets. Specifically, the timing and duration of "on" periods were controlled simply by choosing when and for how long to magnetically stimulate. Rates of delivery during "on" periods were also capable of being remotely regulated by applying different magnetic stimulation frequencies. Applying different stimulation frequencies allowed for different "on" rates initially or could be used to maintain more consistent release rates as the gels became depleted of the drug over time. While the use of these magnetically responsive ferrogels could provide the above-outlined clinical advantages, devices must first be commercially developed to magnetically stimulate implanted ferrogels over a range of frequencies. This could be achieved using simple electromagnets, which have been demonstrated to efficiently regulate mitoxantrone release rates from biphasic ferrogels at stimulation frequencies up to 500 Hz.[37]

Elsewhere, magnetically compressible ferrogels were shown to be capable of delivering molecular payloads after implantation in vivo.[25] In fact, their cyclic magnetic compressions have actually been shown to resist fibrous capsule formation.[36] Previous studies have demonstrated the

DOI: 10.1021/acsbiomaterials.8b00348
ACS Biomater. Sci. Eng. 2018, 4, 2412−2423

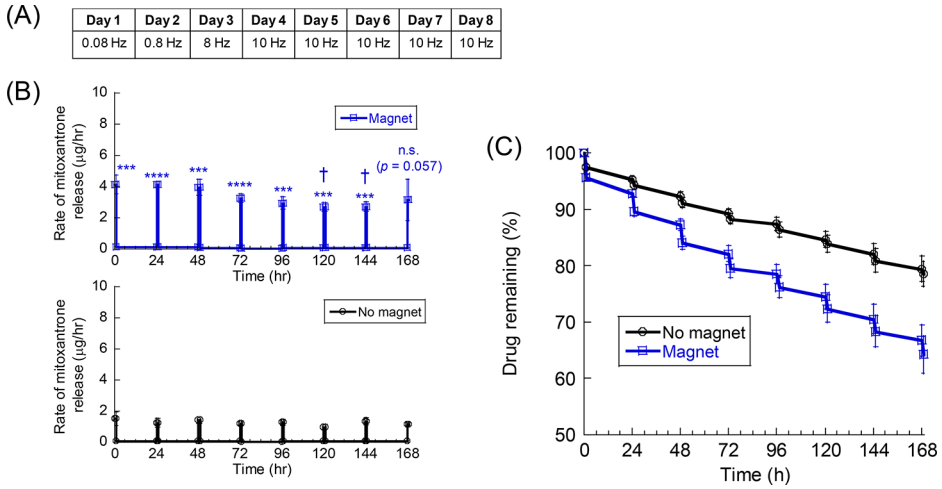

Figure 11. Pulsatile mitoxantrone delivery schedules from ferrogels can be extended beyond 3 days. (A) Table detailing the magnetic stimulation profile used. On each day, 1 h of magnetic stimulation was performed at the indicated frequency. (B) Mitoxantrone release rate vs time when subjected to the magnetic stimulation profile described in part A (blue) compared to controls (black). (C) Percent of mitoxantrone remaining in the gels vs time for magnetically stimulated gels (blue) compared to controls (black). Asterisks indicate levels of statistical differences for given pulse rates compared to controls (see Section 2.8). † indicates that magnetically triggered release rate is statistically lower than triggered rates achieved on other days ($0.03 < p < 0.05$). $N = 4$.

ability to magnetically generate pulsatile mitoxantrone deliveries from ferrogels. Zhao et al.[25] demonstrated that magnetic fields could be used to periodically enhance release rate from magnetically compressible ferrogels when stimulated for 2 min every half hour for 3 h. This resulted in significantly enhanced amounts of release after 3 h compared to controls. The work presented here builds upon the work of Zhao et al. by extending the timeframes of pulsatile release to durations thought to be relevant to chemotherapies and chronotherapies (e.g., days)[19−22] and demonstrating that specific pulsatile deliveries profiles produced by ferrogels have beneficial impact on destroying tumor cell populations. Additionally, by extending these timeframes, magnetic stimulation strategies had to be developed to maintain delivery rates to compensate for drug depletion over time. Finally, this work builds upon previous work by devising strategies for controlling the degree of enhanced delivery rate during magnetic stimulation using the frequency of magnetic stimulation to remotely regulate release rates. Taken altogether, the studies presented here (combined with their in vivo capabilities demonstrated elsewhere) suggest that these magnetically responsive hydrogels could be used to deliver more temporally complex and effective chemotherapeutic delivery profiles to tumor sites in future studies with the degrees of on-demand control needed to (i) experimentally optimize delivery profiles and (ii) clinically alter the course of therapies according to up-to-date prognoses.

5. CONCLUSIONS

These studies demonstrate that pulsatile delivery profiles of a chemotherapeutic (mitoxantrone) are more effective at eliminating melanoma cells than constant (flatline) deliveries of the same integrated dose in vitro. Some pulsatile profiles worked better than others (i.e., schedule s3 was most effective: 24 μg/mL for 2 h during "on" periods, 22 h "off" periods, repeated for 3 days). However, a more complete optimization of delivery profiles will require testing a broader range of delivery profiles in vivo. This work has also demonstrated that a magnetically responsive, biphasic ferrogel can be used to generate pulsatile mitoxantrone delivery profiles similar to those tested on melanoma cells in vitro. The timing of mitoxantrone pulses could be regulated by choosing when to apply magnetic stimuli (i.e., from simple hand-held magnets). The rate of delivery during magnetic stimulation could be regulated by stimulating at different magnetic field frequencies. Thus, these materials could potentially streamline the optimization of pulsatile deliveries by enabling the production of a wide variety of pulsatile profiles directly to tumor sites through on-demand, magnetically triggered stimulations. Finally, these materials could also provide powerful tools for clinically deploying optimized pulsatile delivery profiles at tumor sites while retaining the real-time control needed to alter the course of therapies on-the-fly.

■ ASSOCIATED CONTENT

Supporting Information

The Supporting Information is available free of charge on the ACS Publications website at DOI: 10.1021/acsbiomaterials.8b00348.

Data related to drug loading and rinsing (PDF)

Movie of custom magnetic stimulation setup at 0.1 Hz (AVI)

Movie of custom magnetic stimulation setup at 1 Hz (AVI)

Movie of custom magnetic stimulation setup at 10 Hz (AVI)

■ AUTHOR INFORMATION

Corresponding Author

*E-mail: smkennedy@uri.edu.

ORCID

Stephen M. Kennedy: 0000-0002-7106-2458

Funding

The research reported in this manuscript was supported by an early career development award from the Rhode Island IDeA Network for Biomedical Research Excellence (RI-INBRE) (National Institutes of Health (NIH) National Institute of General Medical Sciences (NIGMS) P20GM103430), Start-up

DOI: 10.1021/acsbiomaterials.8b00348
ACS Biomater. Sci. Eng. 2018, 4, 2412−2423

support from the University of Rhode Island's College of Engineering, a Rhode Island Foundation Medical Research Grant (20144262), a grant from the National Science Foundation (NSF) (CBET-1603433), an NSF Track-2 FEC award (1539068), and a 3 M Company Non-Tenured Faculty Award (32976949).

Notes

The authors declare no competing financial interest.

■ ACKNOWLEDGMENTS

We would like to thank Professor Dr. Everett Crisman for the Zeiss SIGMA VP field emission scanning electron microscope we used to characterize our biomaterial from R.I. Consortium for Nanoscience & Nanotechnology. We would also like to thank Dr. Al Bach and Kim Andrews for their expert advice and giving us easy access to use the xCELLigence system and bright field microscopes from RI-INBRE core facility. Finally, a special thank you to the senior capstone undergraduate engineering students Paul Kintz, Gregory Rosche, and Taylor DiLeo for designing, building, and testing our custom magnetic stimulation setup.

■ REFERENCES

(1) American Cancer Society. *Cancer Facts & Figures 2017*; American Cancer Society: Atlanta, 2017.
(2) Fung, L. K.; Saltzman, W. M. Polymeric implants for cancer chemotherapy. *Adv. Drug Delivery Rev.* **1997**, *26*, 209−230.
(3) Jang, S. H.; Wientjes, M. G.; Lu, D.; Au, J. L. S. Drug delivery and transport to solid tumors. *Pharm. Res.* **2003**, *20*, 1337−1350.
(4) Kearney, C. J.; Mooney, D. J. Macroscale delivery systems for molecular and cellular payloads. *Nat. Mater.* **2013**, *12*, 1004−1017.
(5) Vernon, B.; Wegner, M. Controlled Release. In *Encyclopedia of Biomaterials and Biomedical Engineering*, 1st ed; Wnek, E., Bowlin, G., Eds.; Marcel Dekker AG: New York, 2004; Vol. *1*, pp 384−391.
(6) Brudno, Y.; Mooney, D. J. On demand drug delivery from local depots. *J. Controlled Release* **2015**, *219*, 8−17.
(7) Alam, S.; Baldwin, J.; Tombros, A.; Rinchart, B.; Shields, C.; Swann, M. The single-rod contraceptive implant,. *Clinical proceedings from association of reproductive health professionals* **2008**, 7−9.
(8) U.S. Food and Drug Administration. *IMPLANON (etonogestrel implant)*; Merck & Co., Inc.: 2017.
(9) Acharya, G.; Park, K. Mechanisms of controlled drug release from drug-eluting stents. *Adv. Drug Delivery Rev.* **2006**, *58*, 387−401.
(10) Mani, G.; Feldman, M. D.; Patel, D.; Agrawal, C. M. Coronary stents: A materials perspective. *Biomaterials* **2007**, *28*, 1689−1710.
(11) Chan-Seng, D.; Ranganathan, T.; Zhang, X.; Tang, Y.; Lin, Q.; Kleiner, L.; Emrick, T. Aliphatic polyester terpolymers for stent coating and drug elution: Effect of polymer composition on drug solubility and release. *Drug Delivery* **2009**, *16*, 304−311.
(12) Watson, N.; Kiziltepe, T.; Eavarone, D.; Sasisekharan, R.; Capila, I.; Sengupta, S.; Zhao, G. Temporal targeting of tumour cells and neovasculature with a nanoscale delivery system. *Nature* **2005**, *436*, 568−572.
(13) Attenello, F.; Mukherjee, D.; Datoo, G.; Mcgirt, M.; Bohan, E.; Weingart, J.; Olivi, A.; Quinones-Hinojosa, A.; Brem, H. Use of Gliadel (BCNU) Wafer in the Surgical Treatment of Malignant Glioma: A 10-Year Institutional Experience. *Ann. Surg. Oncol.* **2008**, *15*, 2887−2893.
(14) Westphal, M.; Hilt, D. C.; Bortey, E.; Delavault, P.; Olivares, R.; Warnke, P. C.; Whittle, I. R.; Jääskeläinen, J.; Ram, Z. A phase 3 trial of local chemotherapy with biodegradable carmustine (BCNU) wafers (Gliadel wafers) in patients with primary malignant glioma. *Neuro Oncol.* **2003**, *5*, 79−88.
(15) U.S. Food and Drug Administration. *ZOLADEX (goserelin acetate implant) 10.8 mg*; AstraZeneca Pharmaceuticals LP: 2013.
(16) Gautschi, P.; Frey, P.; Zellweger, R. Bone morphogenitic proteins in clinical applications. *ANZ. J. of Surg.* **2007**, *77*, 626−631.
(17) Kleiner, L. W.; Wright, J. C. Application of Biomaterials: Implants and Inserts. In *Biomaterials Science: An Introduction to Materials in Medicine*, 3rd ed.; Ratner, B. D., Hoffman, A. S., Schoen, F. J., Lemons, J. E., Eds.; Academic Press: Waltham, MA, 2013; pp 1062−1068.
(18) Peppas, N. A.; Leobandung, W. Stimuli-sensitive hydrogels: ideal carriers for chronobiology and chronotherapy. *J. Biomater. Sci., Polym. Ed.* **2004**, *15*, 125−144.
(19) Mormont, M.; Levi, F. Cancer chronotherapy: Principles, applications, and perspectives. *Cancer* **2003**, *97*, 155−169.
(20) Mormont, M. C.; Lévi, F. Circadian-system alterations during cancer processes: a review. *Int. J. Cancer* **1997**, *70*, 241−247.
(21) Cara, S.; Tannock, I. Retreatment of patients with the same chemotherapy: Implications for clinical mechanisms of drug resistance. *Ann. Oncol.* **2001**, *12*, 23−27.
(22) Goldman, A.; Majumder, B.; Dhawan, A.; Ravi, S.; Goldman, D.; Kohandel, M.; Majumder, P. K.; Sengupta, S. Temporally sequenced anticancer drugs overcome adaptive resistance by targeting a vulnerable chemotherapy-induced phenotypic transition. *Nat. Commun.* **2015**, *6* (6139), 1−13.
(23) Ahmed, E. M. Hydrogel: Preparation, characterization, and applications: A review. *J. Adv. Res.* **2015**, *6*, 105−121.
(24) Kennedy, S.; Bencherif, S.; Norton, D.; Weinstock, L.; Mehta, M.; Mooney, D. J. Rapid and Extensive Collapse from Electrically Responsive Macroporous Hydrogels. *Adv. Healthcare Mater.* **2014**, *3*, 500−507.
(25) Zhao, X.; Kim, J.; Cezar, C. A.; Huebsch, N.; Lee, K.; Bouhadir, K.; Mooney, D. J. Active scaffolds for on-demand drug and cell delivery. *Proc. Natl. Acad. Sci. U. S. A.* **2011**, *108*, 67−72.
(26) Cezar, C. A.; Kennedy, S. M.; Mehta, M.; Weaver, J. C.; Gu, l.; Vandenburgh, H.; Mooney, D. J. Biphasic Ferrogels for Triggered Drug and Cell Delivery. *Adv. Healthcare Mater.* **2014**, *3*, 1869−1876.
(27) Hu, S.; Liu, T.; Liu, D.; Chen, S. Controlled Pulsatile Drug Release from a Ferrogel by a High-Frequency Magnetic Field. *Macromolecules* **2007**, *40*, 6786−6788.
(28) Edelman, E. R.; Kost, J.; Bobeck, H.; Langer, R. Regulation of drug release from polymer matrices by oscillating magnetic fields. *J. Biomed. Mater. Res.* **1985**, *19*, 67−83.
(29) Hsieh, S. T. D.; Langer, R.; Folkman, J. Magnetic Modulation of Release of Macromolecules from Polymers. *Proc. Natl. Acad. Sci. U. S. A.* **1981**, *78*, 1863−1867.
(30) Hu, S.; Liu, T.; Liu, D.; Chen, S. Nano-ferrosponges for controlled drug release. *J. Controlled Release* **2007**, *121*, 181−189.
(31) Liu, T.; Hu, S.; Liu, T.; Liu, D.; Chen, S. Magnetic-sensitive behavior of intelligent ferrogels for controlled release of drug. *Langmuir* **2006**, *22*, 5974−5978.
(32) Kost, J.; Wolfram, J.; Langer, R. Magnetic enhanced insulin release in diabetic rats. *J. Biomed. Mater. Res.* **1987**, *21*, 1367−1373.
(33) Huebsch, N.; Kearney, C. J.; Zhao, X.; Kim, J.; Cezar, C. A.; Suo, S.; Mooney, D. J. Ultrasound-triggered disruption and self-healing of reversibly cross-linked hydrogels for drug delivery and enhanced chemotherapy. *Proc. Natl. Acad. Sci. U. S. A.* **2014**, *111*, 9762−9767.
(34) Kearney, C. J.; Skaat, H.; Kennedy, S. M.; Hu, J.; Darnell, M.; Raimondo, T. M.; Mooney, D. J. Switchable Release of Entrapped Nanoparticles from Alginate Hydrogels. *Adv. Healthcare Mater.* **2015**, *4*, 1634−1639.
(35) Kennedy, S.; Hu, J.; Kearney, C.; Skaat, H.; Gu, L.; Gentili, M.; Vandenburgh, H.; Mooney, D. J. Sequential release of nanoparticle payloads from ultrasonically burstable capsules. *Biomaterials* **2016**, *75*, 91−101.
(36) Cezar, C. A.; Roche, E. T.; Vandenburgh, H. H.; Duda, G. N.; Walsh, C. J.; Mooney, D. J. Biologic-free mechanically induced muscle regeneration. *Proc. Natl. Acad. Sci. U. S. A.* **2016**, *113*, 1534−1539.
(37) Kennedy, S.; Roco, C.; Deleris, A.; Spoerri, P.; Cezar, C.; Weaver, J.; Vandenburgh, H.; Mooney, D. J. Improved magnetic regulation of delivery profiles from ferrogels. *Biomaterials* **2018**, *161*, 179−189.
(38) Fox, E. J. Mechanism of action of mitoxantrone. *Neurology* **2004**, *63*, S15−S18.

DOI: 10.1021/acsbiomaterials.8b00348
ACS Biomater. Sci. Eng. 2018, 4, 2412−2423

(39) Lévi, F.; Zidani, R.; Misset, J.-L. Randomized multicentre trial of chronotherapy with oxaliplatin, fluorouracil, and folinic acid in metastatic colorectal cancer. *Lancet* **1997**, *350*, 681−86.
(40) Ehninger, G.; Schuler, U.; Proksch, B.; Zeller, K. P.; Blanz, J. Pharmacokinetics and metabolism of mitoxantrone. A review. *Clin. Pharmacokinet.* **1990**, *18*, 365−80.
(41) Cohen, A. A.; Geva-Zatorsky, N.; Eden, E.; Frenkel-Morgenstern, M.; Issaeva, I.; Sigal, A.; Milo, R.; Cohen-Saidon, C.; Liron, Y.; Kam, Z.; Cohen, L.; Danon, T.; Perzov, N.; Alon, U. Dynamic proteomics of individual cancer cells in response to a drug. *Science* **2008**, *322*, 1511−1516.
(42) Janes, K. A.; Albeck, J. G.; Gaudet, S.; Sorger, P. K.; Lauffenburger, D. A.; Yaffe, M. B. A systems model of signaling identifies a molecular basis set for cytokine-induced apoptosis. *Science* **2005**, *310*, 1646−1653.

DOI: 10.1021/acsbiomaterials.8b00348
ACS Biomater. Sci. Eng. 2018, 4, 2412−2423